High-Efficiency Multijunction Solar Cells

Frank Dimroth and Sarah Kurtz

Abstract

The efficiency of a solar cell can be increased by stacking multiple solar cells with a range of bandgap energies, resulting in a multijunction solar cell with a maximum theoretical efficiency limit of 86.8%. III–V compound semiconductors are good candidates for fabricating such multijunction solar cells for two reasons: they can be grown with excellent material quality; and their bandgaps span a wide spectral range, mostly with direct bandgaps, implying a high absorption coefficient. These factors are the reason for the success of this technology, which has achieved 39% efficiency, the highest solar-to-electric conversion efficiency of any photovoltaic device to date. This article explores the materials science of today's high-efficiency multijunction cells and describes challenges associated with new materials developments and how they may lead to next-generation, multijunction solar cell concepts.

Introduction

As described in the introductory article by Slaoui and Collins, the photovoltaic (PV) industry is growing rapidly. A key strategy for increasing the industry growth is to reduce the amount of high-purity semiconductor material needed to make a solar cell by either thinning the active layers (shrinking the cell vertically) or using optics to focus the light on small solar cells (shrinking the cell laterally) (see Figure 1). If the semiconductor cost can be reduced to a small fraction of the system cost, then increasing the efficiency of the solar cell will add value to the rest of the system without changing the cost appreciably. In this case, higher-efficiency solar cells provide a pathway to lower cost even if the solar cell itself is more expensive. This concept of high-concentration photovoltaics is being pursued by companies around the world.[1]

To date, the highest solar-to-electric conversion efficiency achieved for any PV device is 39% under ~240 suns concentration.[2] One sun is defined as 1 kW/m^2. The basis of this technology is a dual-junction GaInP/GaAs solar cell that was originally invented and developed at the National Renewable Energy Laboratory. Today, triple-junction $Ga_{0.5}In_{0.5}P/Ga_{0.99}In_{0.01}As/Ge$ cells with an additional Ge junction are in production for space applications at Spectrolab, EMCORE, and AZUR Space Solar Power. Its high power-to-mass ratio outweighs its higher cost and drives the success of this solar cell technology in space. Such cells power the Mars Exploration Rovers, Spirit and Opportunity, and are the product of choice for most of today's advanced satellites. Some requirements for space solar cells can be found in Reference 3.

These successful space cells are too expensive to be used in flat-plate terrestrial photovoltaic systems. So, many companies are now developing concentrator systems to enable the use of these cells on earth. This article describes the physics behind these cells, emphasizing the value of combining multiple high-quality materials. We discuss the material characteristics that imply high quality and strategies for making alloys with a range of bandgaps and assembling these into high-efficiency solar cells.

Theoretical Considerations

The theoretical efficiency limits for solar cells can be estimated in a number of ways, ranging from the constraint placed by the second law of thermodynamics to realistic models. In 1961, Shockley and Queisser[4] described the detailed-balance limit of efficiency for *p–n* junction solar cells, balancing the radiative transfer between the sun and the solar cell modeled as black bodies. They calculated an efficiency limit of ~31% for a 1.3-eV material under a 1-sun configuration and ~41% for a 1.1-eV material when the light is maximally concentrated.[4] This calculation assumes an index of refraction of unity for the medium connecting the black bodies. The exact values change with the spectrum. The detailed-balance method gives efficiency limits; realistic models use band-structure properties of known materials and are more relevant to practical applications.

Shockley and Queisser assumed a single *p–n* junction, but the efficiency is increased if multiple materials are used, as illustrated in Figure 2, which shows the solar energy that can be theoretically used by single- and triple-junction cells. In the multijunction solar cell, the thermalization of hot carriers is reduced through the use of high-bandgap materials for the top *p–n* junctions. At the same time, transmis-

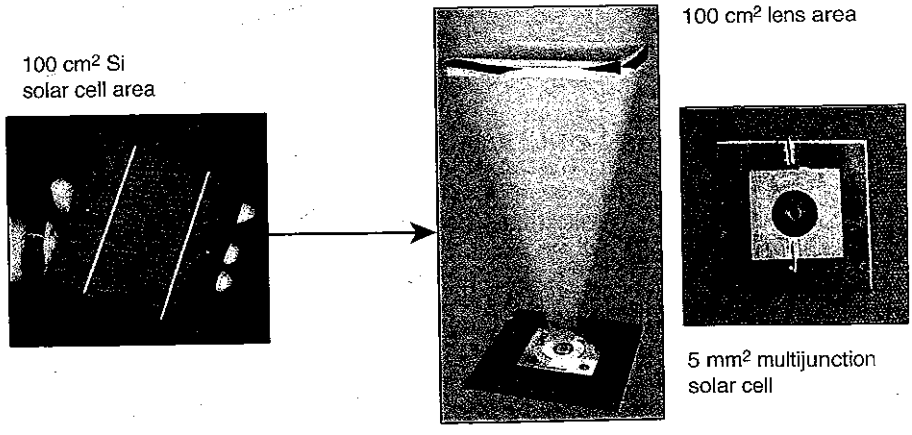

Figure 1. Concentrators are a strategy for reducing the semiconductor material in photovoltaic cells. Typical concentration ratios are 30–1000.

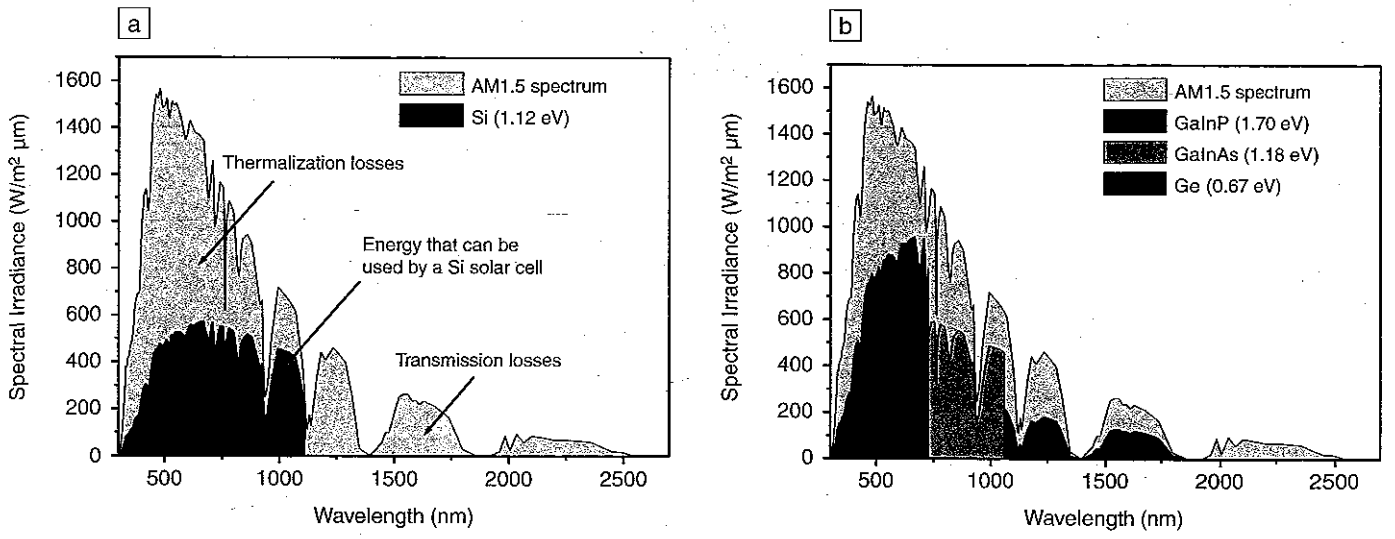

Figure 2. The AM1.5 solar spectrum and the parts of the spectrum that can, in theory, be used by (a) Si solar cells and (b) $Ga_{0.35}In_{0.65}P/Ga_{0.83}In_{0.17}As/Ge$ solar cells.

sion losses of low-energy photons are reduced by using low-bandgap materials for the bottom *p–n* junctions. The detailed-balance approach has been extended[5,6] to describe multijunction cells (Figure 3). The use of multiple materials can increase the efficiency of single-crystal solar cells substantially, but Figure 3 also shows that it is more difficult to realize the benefit of multiple materials when the solar cells are made from polycrystalline or amorphous materials with lower crystal perfection.

Semiconductors with different bandgap energies can be fabricated in a single piece or fabricated separately and then brought together. In a mechanical stack, the different *p–n* junctions are fabricated separately. In a more elegant configuration, the materials with different bandgap energies are grown on top of each other and on a single substrate. In this monolithic device, the different *p–n* junctions are connected in series by interband tunnel diodes, resulting in a final device with one positive and one negative contact. In either case, the materials should be high-quality, as discussed next.

Material Requirements for Best Solar Cell Performance

The performance of a solar cell depends primarily on the dynamics of the minority carriers. Figure 4 of the introductory article in this issue of *MRS Bulletin* shows the basic structure and operation of a generic solar cell. Excess minority carriers are generated when light is absorbed. These carriers diffuse to the built-in field (depletion region) and are separated for use in an outside circuit. Photogenerated carriers (photocarriers) that recombine either at bulk defects or at a surface are lost and do not contribute to electricity production. The achievement of high efficiency requires that the material absorbs the incident solar spectrum and that the photocarriers are separated by the built-in electric field before they recombine. The device design can be optimized to facilitate

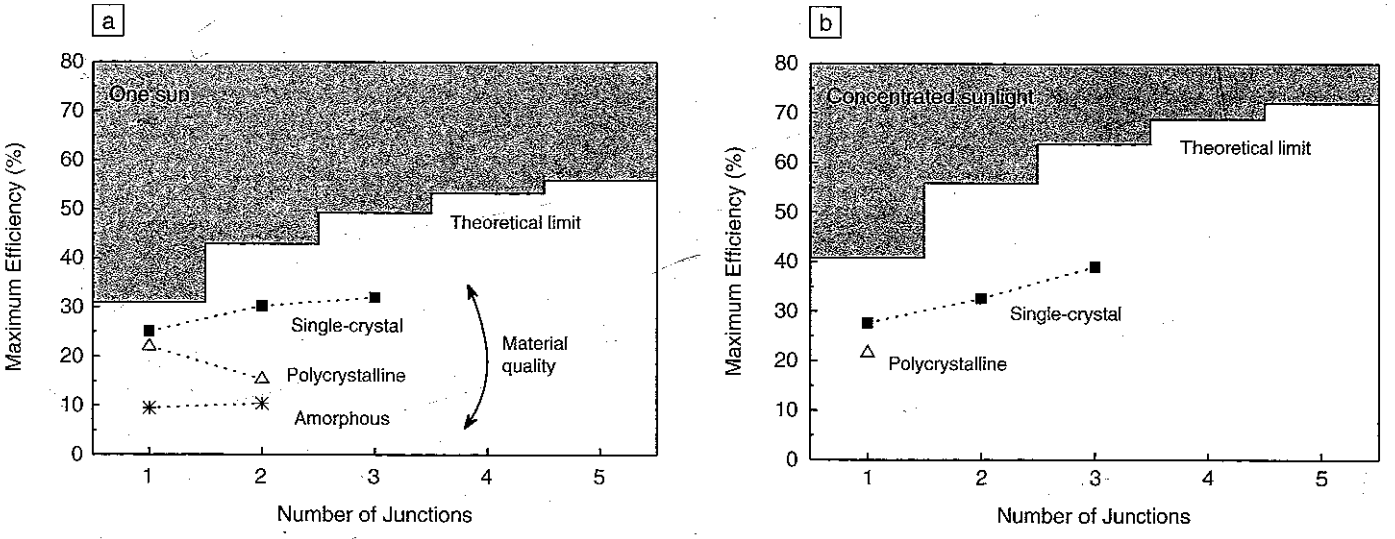

Figure 3. Achieved efficiencies (symbols) and theoretical efficiency limits (solid red lines) estimated by the detailed-balance method as a function of the number of junctions and the structure of the material for (a) 1-sun and (b) concentrated illumination. Higher material quality is correlated with higher efficiency.

the separation of the photocarriers when material quality is poor, as for many low-cost materials. Here, we discuss the material parameters that contribute to or detract from the performance of the solar cell.

The two key material parameters for solar cell operation are minority carrier diffusion length and minority carrier lifetime. The minority carrier diffusion length should be longer than the thickness of the material needed to absorb the light. Indirect-bandgap materials typically have longer minority carrier diffusion lengths, but also require thicker layers to absorb the light. Direct-bandgap materials are usually preferred, because thin layers ($\leq$3 μm) may be adequate to absorb the light. If the material is a uniform single crystal that is free of impurities and defects, there is usually minimal scattering in the cell and the effective carrier mobility will be high, so the achievement of high efficiency relies primarily on achieving long minority carrier lifetimes.

There are three types of electron–hole recombination that can reduce the minority carrier lifetime: Auger, radiative, and nonradiative. Auger recombination involves two photocarriers (two electrons or two holes), with the transfer of the recombination energy to another electron in the conduction band or another hole in the valence band. Thus, Auger recombination is important when the photocarrier concentrations become large, as for indirect-bandgap materials under intense illumination. Radiative recombination is the reverse process of light absorption and is, to some extent, balanced by reabsorption of the emitted light. It is nonradiative recombination caused by defects or impurities that usually makes the difference between high- and low-efficiency solar cells.

The detailed-balance data shown in Figure 3 represent ideal materials with no nonradiative recombination. A review of the efficiencies that have been achieved for crystalline, polycrystalline, and amorphous materials (see Figure 3) demonstrates how the quality of the material can be more important than the number of junctions.

Nonradiative recombination in solar cells is often referred to as Shockley–Read–Hall recombination. The statistics for the trapping of carriers and resulting net recombination are described in Reference 7. They showed that the recombination is fastest in the depletion region, or wherever the Fermi level comes close to the energy of the trap. Shockley and Read showed that deep traps are more likely to act as recombination centers, whereas shallow traps may affect the transport of carriers but are unlikely to catalyze recombination of electron–hole pairs. Thus, it is most important to eliminate deep traps in solar cell materials.

Most mid-gap traps arise from impurities, native point defects, dislocations, grain boundaries, or the surface of the crystal. The semiconductor industry has virtually eliminated crystallographic defects with the growth of high-purity, dislocation-free single crystals of Group IV or III–V materials. The use of II–VI alloys for most semiconductor applications has been less common, probably because native defects have low energies of formation, so that they form easily and are difficult to eliminate. In contrast, III–V materials are known to maintain nearly stoichiometric compositions. For high-quality single crystals of Si or III–V materials, the surfaces are usually the primary source of defects. A higher-bandgap material can passivate the surface by creating a field that repels minority carriers away from the surface, as shown at the back of the solar cell in Figure 4 of the introductory article in this issue.

As already discussed, higher efficiencies may be achieved by using multiple materials with bandgaps that span the solar spectrum. Some of the available material systems are shown in Figure 4, and Figure 5 illustrates four different atomic configurations for fabricating these alloys. For convenience, we assume that the yellow and blue dots in Figure 5 represent Si and Ge atoms, respectively. If every other Si atom is systematically replaced with a Ge atom, then the structure is ordered as shown in Figure 5a, in contrast to a random configuration (Figure 5b). The alloy can also have clusters of Ge atoms taking the shape of quantum wells or dots. The isotropic random structure usually forms naturally during growth of an alloy. It may be impossible to create the ordered structure if it does not form naturally. Quantum well and dot structures require substantial care for excellent quality. Thus, the random structure is usually the easiest to grow.

All four of these types of alloys can tailor the optical properties, as is desired for multijunction cells. However, these structures differ in their scattering of carriers. Alloy scattering reduces the mobility of carriers in random alloys. A perfectly ordered structure avoids alloy scattering and has a mobility that is determined by the band structure. Quantum wells and dots provide absorption of lower-energy photons, but the carriers that are created in these quantum structures tend to be trapped unless the quantum structures are located in the field region. Most studies have shown increased collection when the field is widened to include all quantum structures. As discussed earlier in this section, this wide region encourages nonradiative (Shockley–Read–Hall) recombination. Thus, of the four approaches shown here, the isotropic

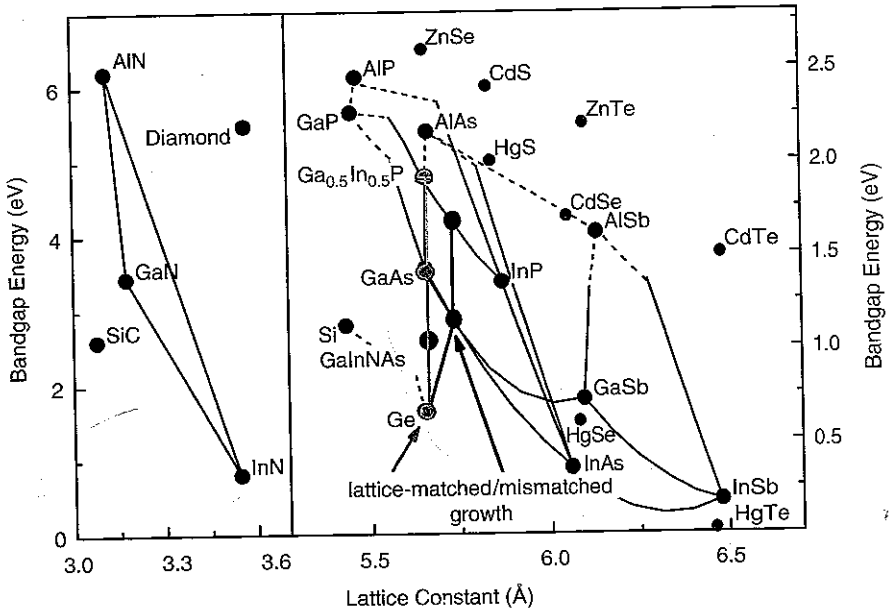

Figure 4. The bandgap as a function of lattice constant for a number of compound semiconductors. The lines indicate data for ternary alloys between binary crystals. Solid lines correspond to direct-bandgap semiconductors, and broken lines to indirect-bandgap semiconductors. The green and blue lines indicate the structures of Figure 6b and 6d, respectively. The black, gray, and red dots indicate binary III–V, II–VI, and a quaternary III–V alloy, respectively.

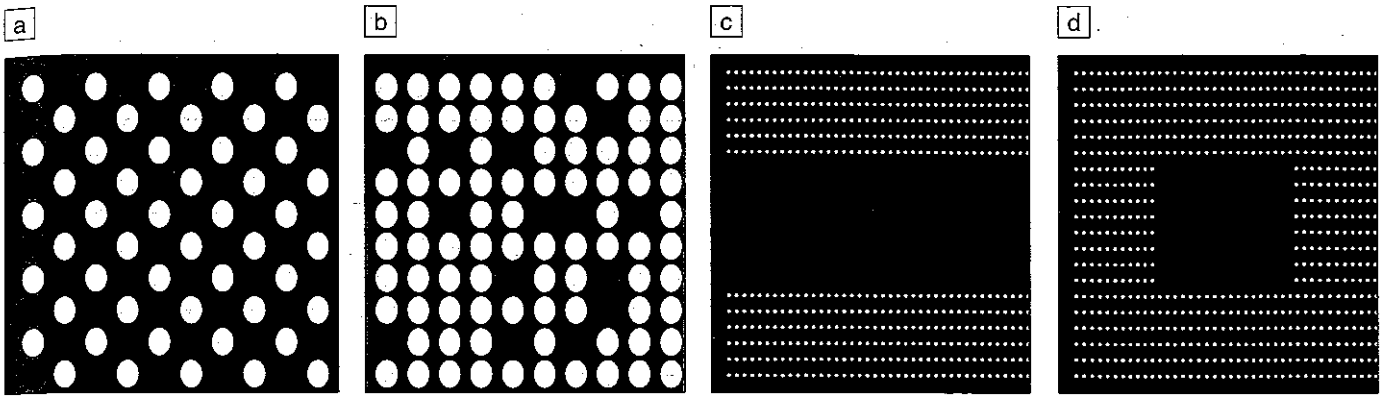

Figure 5. Four ways to assemble single-crystal alloys: (a) ordered, (b) random, (c) quantum wells, and (d) quantum dots. Yellow dots represent Si and blue dots represent Ge.

random structure is advantageous, although other structures are beneficial in specific cases.

Creating even higher-efficiency solar cells in the future involves two steps: (1) selection of a set of materials with bandgaps that span the solar spectrum to provide a high theoretical efficiency, and (2) a method for bringing this set of materials together while retaining excellent material quality. In practice, the second step is more important than the first.

Advanced Multijunction Solar Cell Concepts

There is general consensus in the research community that lattice-matched materials are the easiest to manufacture with high crystal quality. The lattice-matched nature of the $Ga_{0.5}In_{0.5}P/Ga_{0.99}In_{0.01}As/Ge$ (Figure 6a) cell is one of the reasons for its success. Numerous other material combinations have higher theoretical efficiency, but the $Ga_{0.5}In_{0.5}P/Ga_{0.99}In_{0.01}As/Ge$ cell has come closer to its theoretical efficiency limits than any other triple-junction cell. The lattice constants of the materials in this structure are indicated in Figure 4 (green line). The Ge in the $Ga_{0.5}In_{0.5}P/Ga_{0.99}In_{0.01}As/Ge$ structure usually absorbs about the same number of photons as the GaInP and GaInAs layers combined. Thus, theoretically, a higher efficiency would be achieved if a 1-eV material were added between the GaAs and Ge junctions, as shown in Figure 6b. GaInNAs has the desired bandgap (1 eV) and lattice constant (matched to Ge). Unfortunately, the addition of N to GaAs has detrimental effects on the material quality, limiting its utility to approaches that require less photocurrent (e.g., Figure 6c).[8]

A complementary approach for reaching higher efficiencies uses lattice-mismatched materials. The theoretical efficiency of the lattice-matched, triple-junction solar cell is improved by lowering the bandgaps of the first two subcells,[8] with $Ga_{0.35}In_{0.65}P/Ga_{0.83}In_{0.17}As/Ge$ (Figure 6d) approaching the optimal design. This structure uses metamorphic buffer structures between the Ge substrate and the upper cell layers. If the growth conditions for the graded layer are carefully optimized, the relaxation and associated crystallographic defects can be contained within the graded layer, preserving the single-crystal quality of the active layers[9] (see Figure 7). Transmission electron microscopy, showing no threading dislocations in the active solar cell layers and narrow (45 arc sec at half maximum) x-ray diffraction peaks imply a dislocation density of less than 8×10^5 cm^{-2}. The threading dislocation density can be further quantified by cathodoluminescence measured for an epitaxially grown single layer, or by electron-beam-induced current measured for a completed solar cell.

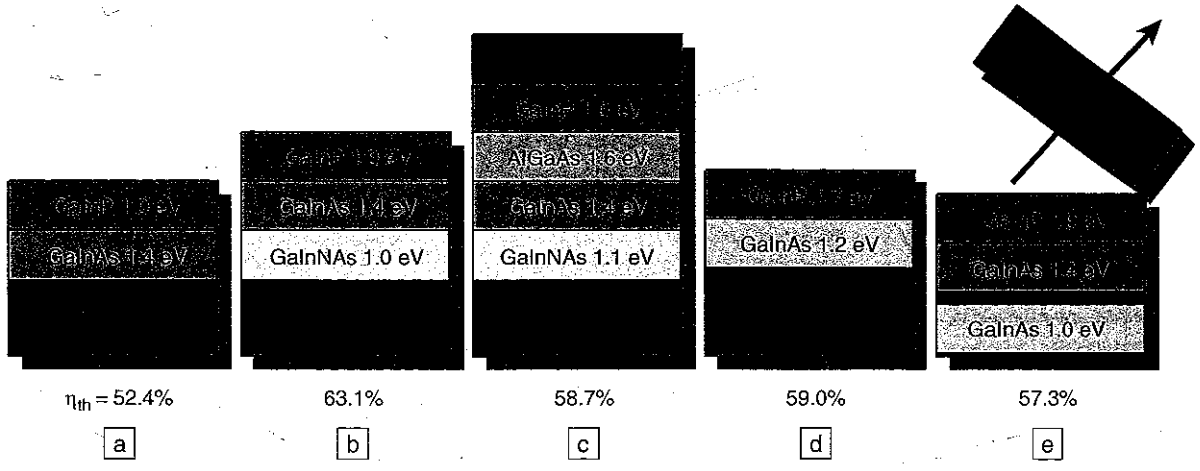

Figure 6. (a)–(e) Advanced high-efficiency multijunction solar cell concepts and their thermodynamic efficiency limits under 500 suns using the AM1.5 direct spectrum. The black bar in (d) and (e) indicates a grading in the lattice constant in these metamorphic approaches. Each subcell consists of a *p–n* junction, front and back surface passivation layers, and the interband tunnel junction, with as many as 50 layers total. In structure (e), all layers are grown upside-down and transferred to a different substrate afterward.

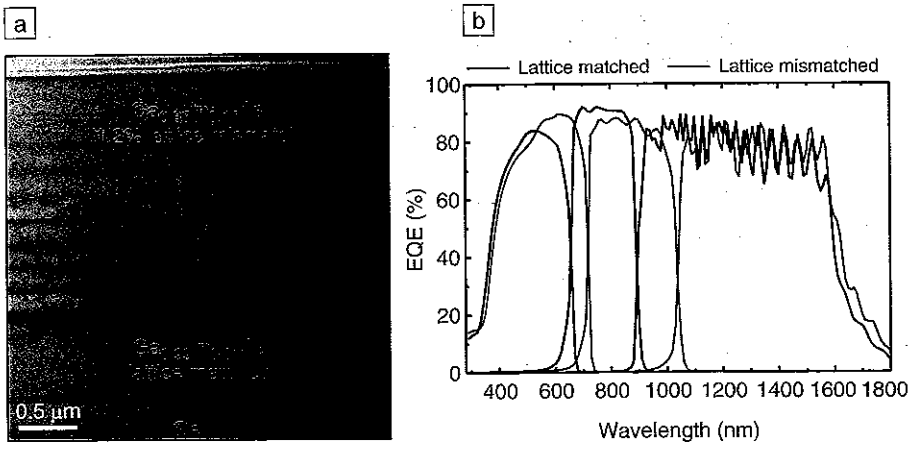

Figure 7. (a) Cross-sectional transmission electron micrograph of a step-graded $Ga_{1-x}In_xAs$ buffer layer grown on Ge. (b) Comparison of the external quantum efficiency (EQE) of a lattice-matched $Ga_{0.5}In_{0.5}P/Ga_{0.99}In_{0.01}As/Ge$ and a lattice-mismatched $Ga_{0.35}In_{0.65}P/Ga_{0.83}In_{0.17}As/Ge$ solar cell. The differences in bandgap energy are clearly visible.

One of the best evaluations of the overall material and interface quality is the solar cell performance itself. The offset between the bandgap of a material, E_g/e, where e is the elementary charge of an electron, and the open-circuit voltage V_{oc} is a good indication of nonradiative recombination losses in the materials.[2] For the lattice-matched growth of a GaAs ($E_g = 1.44$ eV) solar cell, an offset of 387 mV is typically observed. Lattice-mismatched $Ga_{0.83}In_{0.17}As$ ($E_g = 1.18$ eV) solar cells show very similar values of 390 mV, demonstrating their high quality. In contrast, a GaInNAs ($E_g = 1.07$ eV) solar cell loses nearly 600 mV.

The external quantum efficiency (EQE) of a solar cell quantifies the carrier collection efficiency of the p–n junctions. Figure 7 compares the EQE for lattice-matched and lattice-mismatched triple-junction solar cells. Similar values for the EQE have been achieved in both cases. Despite the difficulty of mismatched growth, in recent years metamorphic-solar-cell efficiencies have approached and recently surpassed the best lattice-matched structures. In yet another promising configuration (Figure 6e), $Ga_{0.51}In_{0.49}P$ and GaAs subcells are grown lattice-matched to GaAs or Ge, followed by a grade in the lattice constant and a final $Ga_{0.7}In_{0.3}As$ cell. The substrate only serves as a template for this growth and is later removed to allow illumination of the triple-junction cell from the first-grown side. This cell has already achieved 37.9% efficiency at 10 suns[10] and has the potential to reach efficiencies of >40% in the future.

Summary

The highest-efficiency solar cells use multiple materials with bandgaps spanning the solar spectrum. In these structures, the material quality is more important than the exact bandgap combination in achieving very high efficiencies. GaInP/GaInAs/Ge device efficiencies are nearing 40% and have attracted substantial interest from companies making concentrator systems. A number of advanced approaches include solar cells that integrate new materials (such as the dilute nitrides), accommodate lattice-mismatched growth, and make use of today's most advanced technologies for wafer manipulation. One exciting aspect of multijunction cell development is that there are still many possibilities to explore. The challenge is to achieve the necessary quality in a configuration that makes optimal use of each material. The solar electric conversion efficiency is expected to pass 40% soon and to move toward 50% in years to come. Concentrators will be the platform for making these high-efficiency technologies cost-competitive and enabling continuous cost reductions in the future.

Acknowledgments

The authors appreciate the very helpful contributions of Dr. Andreas Bett and Carsten Baur at Fraunhofer ISE. The writing of this paper was funded under U.S. Department of Energy contract DE-AC36–99G010337 and by the European Commission through the project FULLSPECTRUM (SES6-CT-2003–502620).

References

1. G. Hering, *Photon Int.* (July 2005) p. 50.
2. R.R. King, D.C. Law, C.M. Fetzer, R.A. Sherif, K.M. Edmondson, S. Kurtz, G.S. Kinsey, H.L. Cotal, D.D. Krut, J.H. Ermer, and N.H. Karam, *Proc. 20th Eur. Photovoltaic Solar Energy Conf.* (Barcelona, Spain, 2005) p. 118.
3. S.G. Bailey, R. Raffaelle, and K. Emery, *Prog. Photovolt. Res. Appl.* **10** (2002) p. 399.
4. W. Shockley and H.J. Queisser, *J. Appl. Phys.* **32** (1961) p. 510.
5. A. Marti and G.L. Araujo, *Sol. Energy Mater. Sol. Cells* **43** (1996) p. 203.
6. A.S. Brown and M.A. Green, *Prog. Photovolt. Res. Appl.* **10** (2002) p. 299.
7. W.B. Shockley and W.T.J. Read, *Phys. Rev.* **87** (5) (1952) p. 835.
8. F. Dimroth, *Phys. Status Solidi C* **3** (3) (2006) p. 373.
9. A.W. Bett, C. Baur, F. Dimroth, J. Schöne, *Mater. Res. Soc. Symp. Proc.* **836** (2005) L6.4.1.
10. M. Wanlass, P. Ahrenkiel, D. Albin, J. Carapella, A. Duda, K. Emery, D. Friedman, J. Geisz, K. Jones, A. Kibbler, J. Kiehl, S. Kurtz, W. McMahon, T. Moriarty, J. Olson, A. Ptak, M. Romero, and S. Ward, *Proc. WCPEC-4* (Waikoloa, Hawaii, 2006) p. 729. □